



Contents lists available at ScienceDirect

Optik

journal homepage: [www.elsevier.com/locate/ijleo](http://www.elsevier.com/locate/ijleo)

Original research article

## Bilayer number driven changes in polarizability and optical property in ZnO/TiO<sub>2</sub> nanocomposite films prepared by ALD

S.S. Fouad<sup>a</sup>, B. Parditka<sup>b</sup>, M. Nabil<sup>c</sup>, E. Baradács<sup>b,d</sup>, S. Negm<sup>c</sup>, H.E. Atyia<sup>a,\*</sup>, Z. Erdélyi<sup>b</sup>

<sup>a</sup> Department of Physics, Faculty of Education, Ain Shams University, Cairo, 11566, Egypt

<sup>b</sup> Department of Solid State Physics, Faculty of Sciences and Technology, University of Debrecen, P.O. Box 400, H- 4002, Debrecen, Hungary

<sup>c</sup> Department of Mathematical and Physical Engineering, Faculty of Engineering (Shoubra), Benha University, Cairo, Egypt

<sup>d</sup> Department of Environmental Physics, Faculty of Sciences and Technology, University of Debrecen, H-4026, Debrecen, Poroszlay u. 6, Hungary

### ARTICLE INFO

#### Keywords:

Atomic layer deposition  
Optical energy gap  
Linear refractive index  
Polarizability  
Electrical susceptibility

### ABSTRACT

Samples of ZnO/TiO<sub>2</sub> bilayer films with various layer thickness were fabricated by atomic layer deposition (ALD). The X-ray diffraction (XRD) patterns revealed the absence of sharp peaks and confirms the amorphous nature of the samples under study. The absorption spectra of ZnO/TiO<sub>2</sub> for the three samples were obtained in view of incident wavelength range (350–700 nm). The absorption spectra were used to determine the optical energy band gap. The experimental results show that the direct optical band gap ( $E_g$ ) grown on glass substrate was obviously affected by the increase of the number of ZnO/TiO<sub>2</sub> bilayers and found to decrease from (3.45 to 2.96 eV). The transition power factor ( $P_f$ ) for the three samples was applied to confirm the direct optical transition. A suitable relationship between the linear refractive index ( $n_0$ ) and the optical energy band gap ( $E_g$ ) determined from the experimental and theoretical data was proposed for providing good basis for predication the metallization and polarizability criterion and other related parameters, such as optical dielectric constant and electrical susceptibility. The deep analysis of the studied properties, based on the variation of the number of the bilayer of ZnO/TiO<sub>2</sub>, makes the incorporation of these two materials promising candidates in various optoelectronic applications and solar cell devices.

## 1. Introduction

Transparent conductive oxides (TCOs), exhibit remarkable differences in optical and electrical properties in thin film form when compared to their bulk form. Atomic layer deposition (ALD) method is considered as a great deposition technique for producing high quality thin films due to its self-limited surface reaction behavior and low level of impurity contamination [1–3]. ALD play a role in creating materials with wave guide properties due to the high uniformity of the (ALD) grown films [4,5]. Among all the modern applications for electronic devices, the (ALD) became interesting for new applications of oxides such as TiO<sub>2</sub>, Al<sub>2</sub>O<sub>3</sub>, and ZnO in different areas including biomaterials, photo catalysis and food packaging [6–9]. The (ALD) has proved to be a reliable technique for producing monolayers with well controlled physical and chemical properties [10–12]. Among various TCO materials, ZnO is one of the most important multifunctional oxides of wide gap (3.37 eV) and a large excitation binding energy (60 meV) due to its superior optical

\* Corresponding author.

E-mail address: [hebaelghrip@hotmail.com](mailto:hebaelghrip@hotmail.com) (H.E. Atyia).

<https://doi.org/10.1016/j.ijleo.2021.166617>

Received 3 December 2020; Received in revised form 18 February 2021; Accepted 19 February 2021

Available online 22 February 2021

0030-4026/© 2021 Elsevier GmbH. All rights reserved.

and electronic properties [13–15]. Recently ZnO based films have received much attention because they have advantages over commonly used tin based oxide films [16]. The incorporation of ZnO with TiO<sub>2</sub> is of great significance for improving physical and optical characteristics [16–18]. In the present work a precise study is paid to probe the effect of the thickness of the bilayers on the absorption spectra in terms of the optical energy gap of the ZnO/TiO<sub>2</sub> bilayer number grown by ALD technique. The obtained results are correlated with the linear refractive index, the metallization and the polarizability criterion. In the present work we focus on the effects of the number of ZnO/TiO<sub>2</sub> bilayers on the optical energy gap by studying the absorption spectra in detail. The obtained results are correlated with the linear refractive index, the metallization and the polarizability criterion. It has been found that the linear refractive index, the molar refractive index, the electronic polarizability and the optical dielectric properties are greatly improved by the increase of the number of the ZnO/TiO<sub>2</sub> bilayers.

## 2. Experimental details

The deposition was done using a Beneq TFS-200-186, flow type ALD system. The ALD cycle of sample S1 [20 nm ZnO / 20 nm TiO<sub>2</sub>] consisted of 115 subcycles of ZnO deposition and 286 subcycles of TiO<sub>2</sub> deposition. During the ZnO deposition both precursors (DEZ and H<sub>2</sub>O) were pulsed for 100 ms and was followed by 3 s purge in each case. In case of the deposition of the TiO<sub>2</sub> layer the precursors (TiCl<sub>4</sub> and H<sub>2</sub>O) were pulsed for 100 and 150 ms respectively and was followed by 3 s purge each. During the deposition of the first ZnO layer the NOV and NOP were set to be 300 sccm, while for the TiO<sub>2</sub> deposition the NOV and NOP were set to be 250 and 600 sccm respectively. In order to let the system to stabilize in between the two deposition stages 10 s wait time were included. The samples were deposited at 200 °C. The pressure in the reactor (Pr) and in the surrounding chamber (Pch) were 1 and 9 mbar respectively. For S2 [(20 nm ZnO / 20 nmTiO<sub>2</sub>)x2]and S3[(20 nm ZnO / 20 nmTiO<sub>2</sub>)x5] this two-step process were multiplied for 2 and 5 times. The X-Ray diffraction (XRD) pattern of ZnO/TiO<sub>2</sub> samples were recorded and characterized by using a Shim ADZU diffractometer type XRD 6000. The optical absorption was measured using a V-670 Jasco double-beam spectrophotometer, which utilizes a unique, single monochromator design covering a wavelength range from 190 to 2700 nm.

## 3. Results and discussion

### 3.1. X-ray diffraction (XRD)

The XRD patterns for S1, S2 and S3 are presented in Fig. 1. The obtained pattern is in agreement with the literature at our deposition temperature of 200 °C and shows no sign of either the anatase or the rutile phase of TiO<sub>2</sub> [19]. Considering the ZnO counterpart however, there is a slightly visible peak at around 34.4°, that according to the literature with orientation of (002) of ZnO, that can be attributed to either the very small size of the crystallites or the very small amount of them present in the sample [20–22].

### 3.2. Absorption (A) and optical energy gap (Eg)

Absorption spectroscopy is a powerful technique for exploring optical properties of any materials [23]. Fig. 2 presents the optical absorption spectra (A) for the three samples S1, S2 and S3 in the wavelength range of 350–700 nm. The absence of sharp peaks in the absorption curves seen in Fig. 2 also confirms the very small size of crystallites that had been seen in the X-ray diffraction patterns shown in Fig. 1.

As observed in Fig. 3. The optical energy gap (Eg) can be derived from the well-known relation [24].

$$ah\nu = A(h\nu - E_g)^{P_F} \quad (1)$$

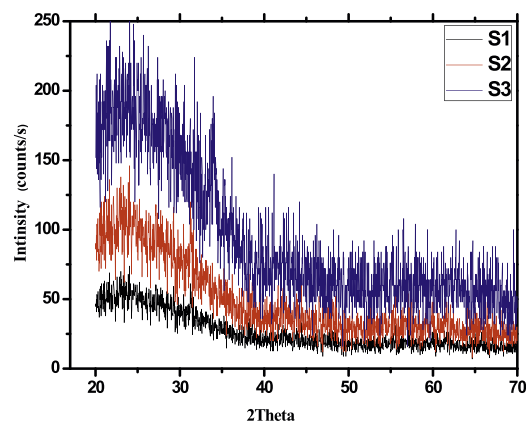


Fig. 1. Shows that the XRD pattern for ZnO/TiO<sub>2</sub> samples S1, S2 and S3.

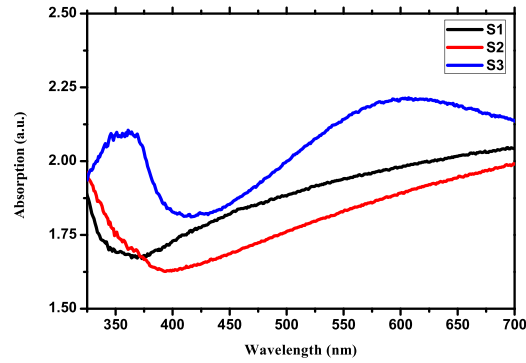


Fig. 2. Shows that the absorption band for TiO<sub>2</sub>/ZnO samples S1, S2 and S3.

Where  $h\nu$ ,  $E_g$  and  $A$  denote the photon energy, the optical energy gap and the band tailing parameter.  $P_F$  in the above equation is the power factor of the transition mode;  $P_F = \frac{1}{2}$  for direct allowed transition,  $P_F = 2$  for indirect allowed transition. The value of  $E_g$  can be estimated from the intercept of the extrapolation of the linear part of the curve to zero absorption with photon energy as seen in Fig. 3. The obtained values of  $E_g$  for the direct allowed transition of S1, S2 and S3 in comparison with the optical energy gap of pure TiO<sub>2</sub> and ZnO given in [25] are presented in Table 1. It is observed that the value of the optical energy gap ( $E_g$ ) decreases with the increase bilayer number for S1, S2 and S3.

This observation implies that the optical gap values are affected by the number of bilayers within the samples. In order to verify the ability of the optical transition whether it becomes direct or indirect we used the following equation [26–28].

$$\ln(\alpha h\nu) = \ln A + P_F \ln(h\nu - E_g) \quad (2)$$

The calculated values of the transition power factor ( $P_F$ ) of S1, S2 and S3 determined from the slope in the insets of Fig. 3 are tabulated in Table 1. As observed the values of  $P_F$  for the three samples are close to 0.5, which prove the direct allowed transition as mentioned earlier.

The linear refractive index is a fundamental parameter that play an important role in designing optical devices [29].

suggested an equation for calculating the linear refractive index ( $n_0$ ) from the optical energy gap values by using the equation:

$$1 - \frac{n_0^2 - 1}{n_0^2 + 2} = \sqrt{\frac{E_g}{20}} \quad (3)$$

Table 1 present the ( $n_0$ ) values for S1, S2 and S3. As observed the optical band gap values for the three samples decrease with the increase of the linear refractive index. It is also noticed that the values of optical energy gap and the linear refractive index of pure TiO<sub>2</sub> and ZnO deviates from that of S1, S2 and S3. The values of the linear refractive index and the energy gap of the pure oxides have been collected from Ref. [30]. These results indicate that the number of bilayers affects the optical parameters. The above observation can be explained on the basis of Duffy empirical relation that relates the energy gap to the molar fraction ( $R_m$ ) for a large number of oxides [31,32].

$$R_m = \left( \frac{n_0^2 - 1}{n_0^2 + 2} \right) V_m \quad (4)$$

where ( $V_m$ ) is the molar volume. This equation infers the explicit expression for ( $R_m$ ) in respect to  $E_g$ . Eq. (4) can be written by means of Lorentz-Lorentz formula as [33].

$$\sqrt{\frac{E_g}{20}} = \left( 1 - \frac{R_m}{V_m} \right) \quad (5)$$

The above equations were used for calculating the metallization criterion of S1, S2 and S3 on the basis of two independent quantities: its linear refractive index and energy gap in the form  $R_m/V_m$  and  $\sqrt{E_g/20}$ , as seen in Table 1. According to the metallization theory proposed by Herzfeld [34], for the condition  $R_m/V_m = 1$ , the linear refractive index becomes infinite, which corresponds to the metallization of covalent solid materials. Accordingly, the sufficient conditions for producing metallic or nonmetallic solids are  $R_m/V_m \geq 1$  (for metal) or  $R_m/V_m < 1$  (for nonmetal). The large value of  $R_m/V_m$  means a large increase in the width of valence and conduction bands, that causes a narrow band gap. The metallization criterion ( $M$ ) reflects the metallic or non-metallic nature of the material on the basis of its band energy and can be calculated according to the following relation [35]:

$$M = 1 - \frac{R_m}{V_m} \quad (6)$$

The metallization criterion ( $M$ ) as seen in Table 1 decreases with increasing the number of TiO<sub>2</sub>/ZnO bilayers. This decrease indicates that our samples are becoming more metallic with the increase of the number of bilayer. Any decrease as seen from (0.415 to

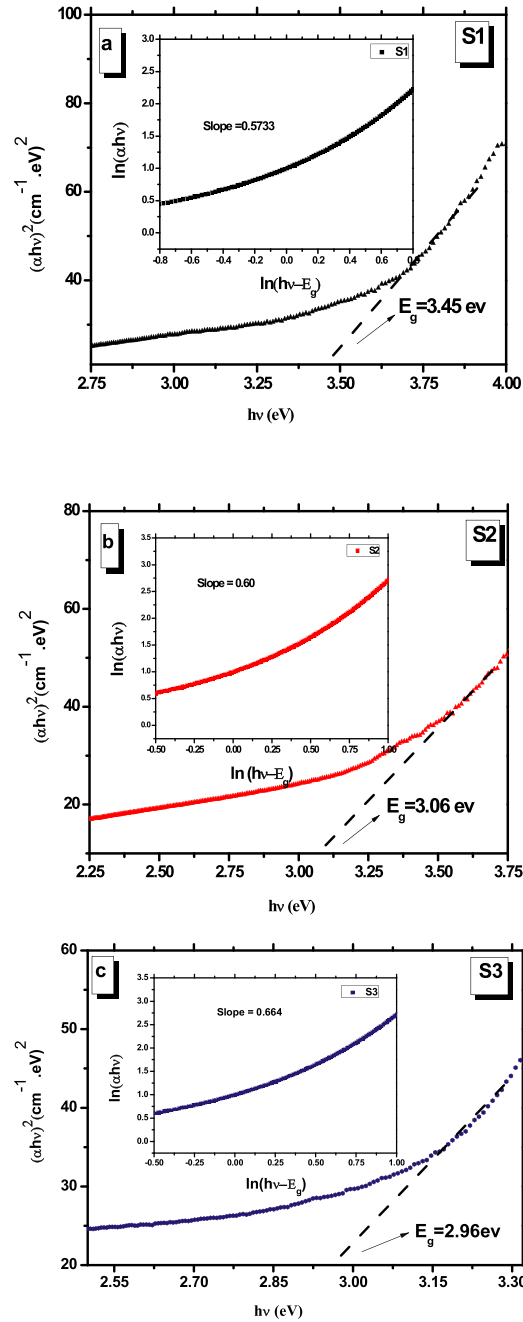


Fig. 3.  $(\alpha h\nu)^2$  versus  $(h\nu)$  plot for samples S1, S2 and S3. The insets show the  $(\ln \alpha h\nu)$  versus  $\ln(h\nu - E_g)$  plots.

0.385) for metallization criterion means a large width in the valence and conduction band, that causes a decrease of the energy gap from (3.45 to 2.96 eV). Briefly, a suitable relationship between the linear refractive index  $n_o$ , energy gap  $E_g$  and the metallization criterion. It has been established that increasing the nonlinear refractive index increases with the increasing linear refractive index and decreasing the energy gap of oxides, and this is related to the increasing the oxides metallicity (see Table 1). An increase in  $R_m/V_m$  from polarizability or metallicity point of view is accompanied by a decrease of the energy band gap. The knowledge of the polarization in different amorphous materials is very interesting because of the need to design optical functional materials with high optical performance such as oxide glasses. The most familiar equation used for the polarizability approach is the Lorentz – Lorentz equation given in Eq. (6). This equation presents the polarizability were the molar fraction ( $R_m$ ) can be expressed as a function of molar polarizability  $\alpha_m$  by ( $R_m = 2.52\alpha_m$ ) were the polarizability increases with the increase of ( $R_m$ ). In short the role of polarizability as basic parameter of linear refractive index and optical energy gap of our oxides samples has been emphasized, where the relationship showed a linear

**Table 1**

The direct optical energy gap ( $E_g$ ), Transition power factor ( $P_F$ ), Linear reflection index ( $n_0$ ),  $R_m/V_m$ , Metallization criterion ( $M$ ) and Electronic polarizability ( $\alpha_e$ ) for the studied ZnO/TiO<sub>2</sub> films with different thickness prepared by the ALD technique.

Estimated Parameter	$E_g$ (eV)	$P_F$	$n_0$	$\frac{R_m}{V_m}$	$\sqrt{E_g/20}$	$M$	$\alpha_e$
Samples							
TiO <sub>2</sub>	3.00	–	2.554	0.35	0.39	0.65	$2.570 \times 10^{-25}$
ZnO	3.40	–	2.008	0.50	0.41	0.50	$1.994 \times 10^{-25}$
S1	3.45	0.5733	2.287	0.585	0.415	0.415	$2.324 \times 10^{-25}$
S2	3.06	0.60	2.381	0.608	0.391	0.392	$2.415 \times 10^{-25}$
S3	2.96	0.664	2.407	0.615	0.384	0.385	$2.440 \times 10^{-25}$

proportionality between the polarizability and the refractive index, and it indicates clearly the linear dependence of  $R_m$  on the polarizability. The electronic polarizability can also be calculated from the linear refractive index using the formula reported in [36].

$$\alpha_e = \frac{3(n_0^2 - 1)}{4\pi N_A(n_0^2 + 2)} \quad (7)$$

where  $N_A$  is the Avogadro's number. The investigated parameters revealed that the linear refractive index and the energy gap, which are associated with the oxides metallicity and polarizability, have strong correlation with the increase of the bilayer number of ZnO/TiO<sub>2</sub>.

### 3.3. Optical dielectric parameters

The dielectric parameters depend mainly on the light absorption of the films and strongly depends on the linear refractive index as well. The dielectric constants are also related to the energy band gap. In this part we calculated the dielectric constant of S1, S2 and S3 by using the simple relation, which is a direct result of Maxwell's equations [37].

$$\epsilon = n_0^2 \quad (8)$$

The relation between the optical dielectric constant and the linear refractive index given in [38] was used for calculating the optical dielectric constant as [39].

$$\epsilon_{opt} = \epsilon - 1 \quad (9)$$

The calculated values of the dielectric constants and the optical dielectric constants of S1, S2 and S3 as presented in Table 2 increases from (5.230–5.793) and (4.230–4.793) respectively. This means that the increase of the number of the bilayers of TiO<sub>2</sub>/ZnO from (1–5) affects the dielectric constants. The increase in the value of the two dielectric constants indicates an increase in the optical absorption, that causes a decrease in the optical energy gap as seen in Table 1. The linear dielectric susceptibility ( $\chi$ ) indicates the ability of a material to become transiently polarized, and it is an important parameter that affects the optical non-linearity of the oxides. The ( $\chi$ ) of S1, S2 and S3 can be calculated by using the relation based on the dielectric constant's values given by [40].

$$\chi = \frac{\epsilon - 1}{4\pi} \quad (10)$$

Table 2 presents the variation values of the electrical susceptibility of S1, S2 and S3. As seen the ( $\chi$ ) value increase from 0.257 to 0.301 with increasing the number of bilayers for S1, S2 and S3. The investigation revealed the linear dependence of the linear refractive index on the dielectric susceptibility.

## 4. Conclusion

The effect of the number of bilayers on the absorption spectra and optical energy gap of the ZnO/TiO<sub>2</sub> system with different thickness for S1-(20 nm/20 nm), S2-(20 nm/20 nm)x2 and S3-(20 nm/20 nm)x5, respectively, prepared by atomic layer deposition (ALD) were investigated. The results demonstrate that the ALD is promising technique to grow thin films with high efficiency and remarkable optical properties. The direct optical band gap and the transition power factor were investigated. The optical band gap was found to decrease with the increase of the number of bilayers of ZnO/TiO<sub>2</sub>. A correlation was observed between the linear refractive index ( $n_0$ ) and the energy band gap ( $E_g$ ) in terms of the metallization criterion, polarizability and dielectric properties on the basis of experimental and theoretical data. The investigations revealed that the linear refractive index is one of the most important factors which are associated with the oxide's metallization. The change in the number of bilayers of ZnO / TiO<sub>2</sub> thin films fundamentally affects the metallization criterion and the polarizability. On these bases it is suggested that ZnO/TiO<sub>2</sub> bilayer thin films prepared by the (ALD) with appropriate thickness makes this technology interesting and quite promising for fabricating materials for nonlinear optics applications.

**Table 2**  
Direct constant ( $\epsilon$ ) and dielectric susceptibility ( $\chi$ ) for the studied ZnO/TiO<sub>2</sub> films with different thickness prepared by the ALD technique.

Estimated Parameter Samples	$\epsilon$	$\epsilon_{opt}$	$\chi$
S1	5.230	4.230	0.257
S2	5.669	4.669	0.292
S3	5.793	4.793	0.301

## Declaration of Competing Interest

The authors report no declarations of interest.

## Acknowledgements

The samples were prepared at Debrecen University, Hungary according to the Erasmus Staff Mobility Agreement, and the agreement between Faculty of Education, Ain Shams University “coordinator and supervisor Prof. Dr. Suzan Fouad “and Faculty of Science and Technology, University of Debrecen “coordinator and supervisor Prof. Dr. Zoltán Erdélyi. The samples were measured at Laser Physics and Nanotechnology Unit (LPTU), Faculty of Engineering Shoubra, Benha University. The research was financed by the Higher Education Institutional Excellence Programme (NKFIH-1150-6/ 2019) of The Ministry of Innovation and Technology in Hungary, within the framework of the Energetic thematic programme of the University of Debrecen.

## References

- [1] G. Torrisi, A. Di Mauro, M. Scuderi, G. Nicotra, G. Embellisher, Atomic layer deposition of ZnO/TiO<sub>2</sub> multilayers: towards the understanding of Ti-doping in ZnO thin films, *RSC Adv.* 6 (91) (2016) 88886–88895.
- [2] Sylvio Schubert, Jan Meiss, Lars Müller-Meskamp, Karl Leo, Improvement of transparent metal top electrodes for organic solar cells by introducing a high surface energy seed layer, *Adv. Energy Mater.* 3 (4) (2013) 438–443.
- [3] Klaus Ellmer, Rainald Mientus, Carrier transport in polycrystalline transparent conductive oxides: a comparative study of zinc oxide and indium oxide, *Thin Solid Films* 516 (14) (2008) 4620–4627.
- [4] Octavio Graniel, Matthieu Weber, S.ébastien Balme, Philippe Miele, Mikhael Bechelany, Atomic layer deposition for biosensing applications, *Biosens. Bioelectron.* 122 (2018) 147–159.
- [5] Muhammad Rizwan Saleem, Rizwan Ali, Mohammad Bilal Khan, Seppo Honkanen, Jari Turunen, Impact of atomic layer deposition to nanophotonic structures and devices, *Front. Mater.* 1 (2014) 18.
- [6] Taewook Nam, Jae-Min Kim, Min-Kyu Kim, Hyungjun Kim, Woo-Hee Kim, Low-temperature atomic layer deposition of TiO<sub>2</sub>, Al<sub>2</sub>O<sub>3</sub>, and ZnO thin films, *J. Korean Phys. Soc.* 59 (2) (2011) 452–457.
- [7] Hanaa Zaka, B. Parditka, Z. Erdélyi, H.E. Atyia, Pankaj Sharma, S.S. Fouad, Investigation of dispersion parameters, dielectric properties and opto-electrical parameters of ZnO thin film grown by ALD, *Optik* 203 (2020), 163933.
- [8] Waldo J.E. Beek, Martijn M. Wienk, RenéA.J. Janssen, Hybrid solar cells from regioregular polythiophene and ZnO nanoparticles, *Adv. Funct. Mater.* 16 (8) (2006) 1112–1116.
- [9] Hanaa Zaka, S.S. Fouad, B. Parditka, A.E. Bekheet, H.E. Atyia, M. Medhat, Z. Erdélyi, Enhancement of dispersion optical parameters of Al<sub>2</sub>O<sub>3</sub>/ZnO thin films fabricated by ALD, *Sol. Energy* 205 (2020) 79–87.
- [10] Yumeng Shi, Henan Li, Lain-Jong Li, Recent advances in controlled synthesis of two-dimensional transition metal dichalcogenides via vapour deposition techniques, *Chem. Soc. Rev.* 44 (9) (2015) 2744–2756.
- [11] Aurore Olivier, Franck Meyer, Jean-Marie Raquez, Pascal Damman, Philippe Dubois, Surface-initiated controlled polymerization as a convenient method for designing functional polymer brushes: from self-assembled monolayers to patterned surfaces, *Prog. Polym. Sci.* 37 (1) (2012) 157–181.
- [12] Yue Li, Guotao Duan, Guangqiang Liu, Weiping Cai, Physical processes-aided periodic micro/nanostructured arrays by colloidal template technique: fabrication and applications, *Chem. Soc. Rev.* 42 (8) (2013) 3614–3627.
- [13] Chenguo Wu, Jie Shen, Jin Ma, Sanpo Wang, Zhuangjian Zhang, Xiliang Yang, Electrical and optical properties of molybdenum-doped ZnO transparent conductive thin films prepared by dc reactive magnetron sputtering, *Semicond. Sci. Technol.* 24 (12) (2009), 125012.
- [14] Agnieszka Kolodziejczak-Radzimska, Teofil Jesionowski, Zinc oxide—from synthesis to application: a review, *Materials* 7 (4) (2014) 2833–2881.
- [15] Teofil Jesionowski, Filip Ciesielczyk (Eds.), *Multifunctional Oxide-Based Materials: From Synthesis to Application*, MDPI, 2019.
- [16] H.Asgari Moghaddam, M.R. Mohammadi, S.M. Seyed Reyhani, Improved photon to current conversion in nanostructured TiO<sub>2</sub> dye-sensitized solar cells by incorporating cubic BaTiO<sub>3</sub> particles delimiting incident, *Sol. Energy* 132 (2016) 1–14.
- [17] Mohammad Reza Delsouz Khaki, Mohammad Saleh Shafeeyan, Abdul Aziz Abdul Raman, Wan Mohd Ashri Wan Daud, Evaluating the efficiency of nano-sized Cu doped TiO<sub>2</sub>/ZnO photocatalyst under visible light irradiation, *J. Mol. Liq.* 258 (2018) 354–365.
- [18] C.A. Orge, J.L. Faria, M.F.R. Pereira, Photocatalytic ozonation of aniline with TiO<sub>2</sub>-carbon composite materials, *J. Environ. Manage.* 195 (2017) 208–215.
- [19] Jina Leem, Inhye Park, Yinshi Li, Wenhao Zhou, Zhenyu Jin, Seokhee Shin, Yo-Sep Min, Role of HCl in atomic layer deposition of TiO<sub>2</sub> thin films from titanium tetrachloride and water, *Bull. Korean Chem. Soc.* 35 (4) (2014) 1195.
- [20] Hisao Makino, Seiichi Kishimoto, Takahiro Yamada, Aki Miyake, Naoki Yamamoto, Tetsuya Yamamoto, *Phys. Stat. Sol.* 8 (2008) 1971–1974.
- [21] Hisao Makino, Aki Miyake, Takahiro Yamada, Naoki Yamamoto, Tetsuya Yamamoto, Influence of substrate temperature and Zn-precursors on atomic layer deposition of polycrystalline ZnO films on glass, *Thin Solid Films* 517 (10) (2009) 3138–3142.
- [22] Swee-Yong Pung, Kwang-Leong Choy, Xianghui Hou, Chongxin Shan, Preferential growth of ZnO thin films by the atomic layer deposition technique, *Nanotechnology* 19 (43) (2008), 435609.
- [23] M. Nabil, Shaimaa A. Mohamed, K. Easawi, Salah S.A. Obayya, S. Negm, H. Talaat, M.K. El-Mansy, Surface modification of CdSe nanocrystals: application to polymer solar cell, *Curr. Appl. Phys.* 20 (3) (2020) 470–476.
- [24] I.M. El Radaf, H.Y.S. Al-Zahrani, S.S. Fouad, M.S. El-Bana, Profound optical analysis for novel amorphous Cu<sub>2</sub>FeSnS<sub>4</sub> thin films as an absorber layer for thin film solar cells, *Ceram. Int.* (2020) 18778–18784.
- [25] S.S. Fouad, G.A.M. Amin, M.S. El-Bana, Physical and optical characterizations of Ge<sub>10</sub>Se<sub>90-x</sub>Te<sub>x</sub> thin films in view of their spectroscopic ellipsometry data, *J. Non. Solids* 481 (2018) 314–320.
- [26] D. Bhattacharyya, S. Chaudhuri, A.K. Pal, Bandgap and optical transitions in thin films from reflectance measurements, *Vacuum* 43 (4) (1992) 313–316.

- [27] Ahmed Saeed Hassanien, Alaa A. Akl, Influence of composition on optical and dispersion parameters of thermally evaporated non-crystalline  $\text{Cd}_{50}\text{S}_{50-x}\text{Se}_x$  thin films, *J. Alloys Compd.* 648 (2015) 280–290.
- [28] E.G. El-Metwally, E.M. Assim, S.S. Fouad, Optical characteristics and dispersion parameters of thermally evaporated  $\text{Ge}_{50}\text{In}_4\text{Ga}_{13}\text{Se}_{33}$  chalcogenide thin films, *Opt. Laser Technol.* 131 (2020), 106462.
- [29] J.A. Duffy, Trends in energy gaps of binary compounds: an approach based upon electron transfer parameters from optical spectroscopy, *J. Phys. C Solid State Phys.* 13 (16) (1980) 2979.
- [30] Vesselin Dimitrov, Sumio Sakka, Linear and nonlinear optical properties of simple oxides. II, *J. Appl. Phys.* 79 (3) (1996) 1741–1745.
- [31] Neelam Berwal, Sunil Dhankhar, Preeti Sharma, R.S. Kundu, R. Punia, N. Kishore, Physical, structural and optical characterization of silicate modified bismuth-borate-tellurite glasses, *J. Mol. Struct.* 1127 (2017) 636–644.
- [32] Ahmed Saeed Hassanien, Studies on dielectric properties, opto-electrical parameters and electronic polarizability of thermally evaporated amorphous  $\text{Cd}_{50}\text{S}_{50-x}\text{Se}_x$  thin films, *J. Alloys Compd.* 671 (2016) 566–578.
- [33] Charles M. Bowden, Mark J. Bloemer, Focus issue: local field effects, *Opt. Express* 1 (6) (1997), 133-133.
- [34] K.F. Herzfeld, On atomic properties which make an element a metal, *Phys. Rev.* 29 (5) (1927) 701.
- [35] Neelam Berwal, Sunil Dhankhar, Preeti Sharma, R.S. Kundu, R. Punia, N. Kishore, Physical, structural and optical characterization of silicate modified bismuth-borate-tellurite glasses, *J. Mol. Struct.* 1127 (2017) 636–644.
- [36] Beena Bhatia, S.L. Meena, Vishal Parihar, Monika Poonia, Optical basicity and polarizability of  $\text{Nd}^{3+}$ -doped bismuth borate glasses, *New J. Glass Ceram.* 5 (03) (2015) 44.
- [37] M.S. El-Bana, S.S. Fouad, Opto-electrical characterization of  $\text{As}_{33}\text{Se}_{67-x}\text{Sn}_x$  thin films, *J. Alloys Compd.* 695 (2017) 1532–1538.
- [38] S.L. Meena, Beena Bhatia, Polarizability and optical basicity of  $\text{Er}^{3+}$  ions doped zinc lithium bismuth borate glasses, *J. Pure Appl. Ind. Phys* 6 (10) (2016) 175–183.
- [39] S.H. Wemple, Refractive-index behavior of amorphous semiconductors and glasses, *Phys. Rev. B* 7 (8) (1973) 3767.
- [40] G. Dresselhaus, MS Dresselhaus proc, *Int. Sch. Phys. Enrico Fermi* 34 (1966) 198.